Experiments in Fluids 6, 305–315 (1988)

Experiments in Fluids

© Springer-Verlag 1988

Vortex ring/viscous wall layer interaction model of the turbulence production process near walls*

C. C. Chu and **R. E. Falco**

Turbulence Structure Laboratory, Dept. of Mechanical Engineering, Michigan State University, East Lansing, MI 48824, USA

Abstract. An experimental simulation of the interaction of vortex ring-like eddies with the sublayer of a turbulent boundary layer is investigated. An artificially generated vortex ring interacting with a Stokes' layer enables investigation of the interaction with reproducible initial conditions and in the absence of background turbulence. All of the observed features in the turbulent boundary layer production process such as the streaky structure, the pockets, the hairpin vortices, streak lift-up, oscillation, and breakup, have been observed to form. The model shows us that hairpin vortices can pinchoff and reconnect forming new vortex ring-like eddies. Interestingly, the model includes interactions that occur with low probability in the turbulent boundary layer, but which contribute significantly to transport, and may be the events most readily controllable.

List of symbols

D	the diameter of a vortex ring
R_θ	Reynolds number based on momentum thickness
T	time to instability
T_p	average time between pockets
U_c	convection velocity
U_r	velocity of a vortex ring
U_{TE}	convection velocity of a Typical eddy
U_w	velocity of the moving belt
u_τ	friction velocity
U_∞	freestream velocity
x	coordinate in the main flow direction
y	coordinate normal to the surface
z	spanwise coordinate
δ	the Stokes' layer thickness
θ	momentum thickness of the shear layer
ν	kinematic viscosity
λ	streamwise wavelength
τ	shear stress
ω_z	spanwise vorticity

Superscripts

$()^+$ non-dimensionalized by ν/u_τ

1 Introduction

There is a need to construct both experimental and numerical simulations of the turbulence production process near walls, because of the difficulty of isolating mechanisms when experiments are conducted in the boundary layer flows. A good simulation must embody the essential features of the production process. In this paper we report a new observation in turbulent boundary layers that helps complete the picture of structural feature interactions, and then present an experimental simulation that models all of the important properties.

Turbulent boundary layer structure that should be modeled includes the long streaks (Runstadler et al. 1963), the pockets (Falco 1980a, 1980b), the hairpins (Falco 1982, Acarlar and Smith 1984), the Typical eddies (Falco 1977, 1983), and coherent regions of streamwise vorticity and/or streamwise vortices. Basically, these structural features have been shown to be associated with the production process, but the formation of the structures and the interactions are not completely understood. A number of investigators have studied the formation of low speed streaks. Oldaker and Tiederman (1977) observed that a pair of low speed streaks formed as a result of the response to what appeared to be a sequence of local high speed outer region eddies interacting with the wall and aligned along a streamwise direction. The path left by the outer region disturbances clearly formed a high speed streak. Falco (1980a) observed the formation of low speed streaks in pairs by a similar mechanism. Although low speed streaks are often observed to exist singly, care must be taken when interpreting low speed streak formation, because once formed the low speed streaks can persist for very long times (Smith and Metzler 1983), and have simply convected into the observation zone.

Since the mid fifties, it has been suggested that long counter rotating streamwise vortices exist in the wall region and that pairs of these vortices produce a gathering of wall layer dye between them that we see as the low speed streaks. A high speed streak would be the result of high speed fluid being induced towards the wall between a pair of these streamwise vortices rotating the other way. A number of authors have suggested causes for these streamwise vortices. The currently most popular sug-

* A version of this paper was presented at the Tenth Symposium on Turbulence, University of Missouri-Rolla, Sept. 22–24, 1986

gestion is that they are the 'legs' of hairpin vortices that are also observed in the wall region. However, as Acarlar and Smith (1984) have pointed out, it is very hard to understand how the hairpin legs could extend upstream as far as would be necessary to produce streaks of length $x^+ = O(1000)$. Thus, there is still no experimental evidence supporting the various rational physical hypotheses describing the formation of long streaks.

Another feature of the wall region structure is the frequent rearrangement of marker that moves it away from a local region, leaving a scoured 'pocket' of low marker concentration. Figure 1 shows two pockets as seen in a layer of smoke marked sublayer fluid. Pockets are footprints of outer region motions that interact with the wall. Falco (1980 a) showed that they start out as a movement of wall layer fluid away from a location as a high speed outer region eddy (a Typical eddy, discussed below), nears the wall. The interaction results in the footprint opening up into a developed pocket shape. Fluid is seen to lift-up from the downstream end of the pocket, and take on the characteristics of a hairpin vortex (Falco 1982).

We have also observed hairpins appearing to form over individual streaks. The streak is seen to become lumpy, and one of the lumps grows and a hairpin emerges from it. Acarlar and Smith (1984) have also observed hairpins growing over simulated streaks, and it appears, in a turbulent boundary layer.

The microscale coherent motions observed across a turbulent boundary layer, which are similar to laminar vortex rings embedded in a shear flow, are called Typical eddies. They have been studied by Falco (1974, 1977, 1982, 1983), who showed that they contribute significantly to the Reynolds stress in the outer part of the boundary layer, and that they are the excitation eddies that create the pockets. Experiments using two mutually orthogonal sheets of laser light enabled Falco (1980 b) to determine, as far as the smoke marking allows, that the coherent feature was a ring, as opposed to a portion of a hairpin vortex, as suggested by Head and Bandyopadhyay (1981).

Both types of hairpin creation mechanisms described above can produce hairpins that can pinch-off and form new vortex rings. Falco (1983) showed visual evidence of a hairpin lifting from the downstream end of a pocket, contorting and pinching off to form a new vortex ring-like Typical eddy. This pinch-off mechanism has also been clearly shown to occur in the calculations of Moin et al. (1986) mentioned above.

Many investigators have noted the presence of streamwise vortices in the wall region. Almost without exception, the vortices have been of short extent (Praturi and Brodkey 1978, Falco 1980 b, Smith 1982). A number of investigators have suggested that streamwise vortices of much greater extent exist in the wall region, essentially laying just above the wall in pairs, which are responsible for the creation of both low and high speed streaks. This evidence is of a statistical nature, usually from correlation measurements. However, no one has ever observed them, and recent calculations of turbulent channel flow using the full Navier-Stokes equations (Kim 1986), have shown that the eddies which have streamwise vorticity are not elongated in the stream direction.

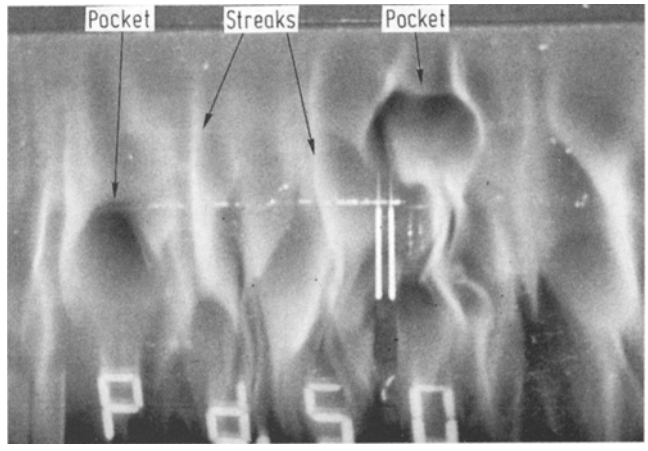

Fig. 1. Two pockets and a pair of streaks as seen in wall slit visualization of the sublayer of a turbulent boundary layer using smoke as the contaminant in air; the slit is at the top of the photo, and the flow is from top to bottom

We will present new boundary layer observations on the formation of streamwise streaks, show that the vortex ring/wall layer simulation can exhibit all of the structural features discussed above, and help us understand their formation and interactions.

2 Experimental techniques

The boundary layer motions were made visible by seeding the flow with 0.5 – 5 micron oil droplets, and illuminating the oil fog with laser light spread into sheets that could be placed parallel to the wall in the wall region, or perpendicular to the wall and parallel to the flow, or both. The technique has been described by Falco (1980 c), so we will not repeat the details here. A new twist, used in these new experiments, which was of particular value in finding the long streaks and their correspondence with the coherent motions above the wall, was the capability to observe the washout of smoke in a laser sheet parallel to the wall while we could simultaneously observe the motion above the wall in a laser sheet perpendicular to the wall and parallel to the flow.

2.1 Vortex ring/moving wall simulations

We can simulate the interaction of a Typical eddy with the viscous wall region of a turbulent boundary layer by creating a vortex ring and having it convect towards or away from a moving wall. For convenience, we have used an impulsively started wall. It has the advantages of being

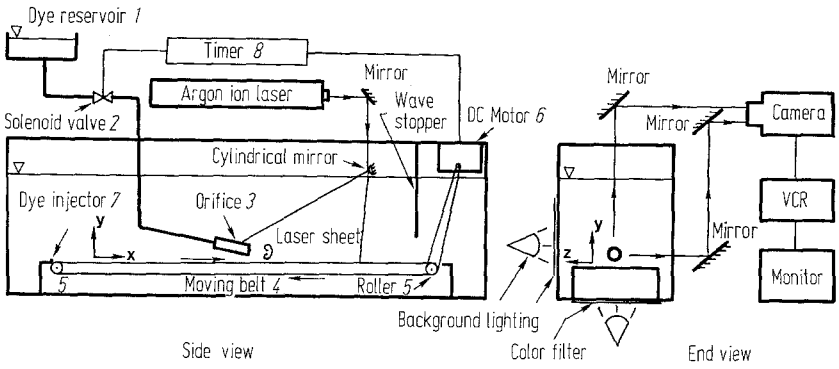

Fig. 2. Side and end views of a schematic of the experimental apparatus used in the vortex ring/moving wall simulations

an exact solution of the Navier-Stokes equations (Stokes' first problem), and therefore is well defined. Furthermore, the velocity profile is approximately linear in the wall region which is similar to the mean velocity profile of the viscous sublayer of a turbulent boundary layer. It is relatively easy to match the friction velocity in these simulations with those found in low Reynolds number turbulent boundary layers. We can also match the Reynolds number and relative convection velocity of the Typical eddies.

Experimental simulations were performed in a water tank which is 0.41 m deep by 0.32 m wide by 2.44 m long. Figure 2 shows the side view and end view of the experimental apparatus which includes a vortex ring generating device, a moving belt and driving arrangement, a synchronizing timer, and visualization recording devices.

The vortex ring generating device includes a constant head reservoir from which fluid, which could be dyed, passes through a solenoid valve whose opening time could be varied, and an orifice of prescribed size (Fig. 2, items *1*, *2*, and *3*). The constant head reservoir (item *1*) is filled with a mixture of 10 ppm Fluorescent Sodium Salt Sigma No. F-6377 green dye and water solution. As the solenoid valve (*2*) opens, a slug of dyed fluid is released from the orifice (*3*) by the pressure head, and rolls up into a vortex ring. Three different inner diameters of the orifice have been used: 2.54 cm, 1.27 cm, and 0.95 cm. The size and speed of the vortex ring generated depends upon both the height of the dye reservoir and the opening duration time of the solenoid valve for a fixed orifice. The details were discussed in Liang (1984).

The wall upon which the vortex ring interacted is actually a moving belt (*4*) made of transparent plastic which has a smooth surface. Two ends of the belt are joined together to form a loop, which circulates around two rollers (*5*) as shown in Fig. 2. The width of the belt is 17.8 cm; and the distance between the two rollers is 152.4 cm. The test section is at 76.2 cm downstream from one of the rollers, giving us a Stokes' layer for this distance (if the belt is run longer, Blasius effects begin to enter into the problem). This width/length ratio is sufficient to prevent the disturbances generated in the corners from reaching the center of the belt at the test section. Therefore, the wall layer flow on the moving belt could be considered two-dimensional. One of the rollers is driven by a 1/4 hp DC motor (*6*). The speed of the belt is adjustable within the range of 2.5 cm/s to 22.9 cm/s. The belt reaches a constant speed very soon (within a second) after power is turned on. This short acceleration period allows us to consider the belt to be impulsively started. As the belt moves, a Stokes' layer builds up on the belt. A mixture of red food coloring and water is used to mark the wall layer for visualization. The belt is covered with dye before each run during a 'dye run' using a dye injector near the leading roller of the belt, shown in Fig. 2 (*7*). The fluid is allowed to come to complete rest before each 'data run'.

The opening duration time of the solenoid valve, and the time delay between the onset of the belt movement and release of the vortex ring, are controlled by a 115 VAC/60 Hz timer designed in the laboratory. Since the thickness of the Stokes' layer, δ, is a function of the square root of the belt run time, by carefully adjusting the time delay, we can adjust δ/D as desired.

The primary visual data consisted of simultaneous plan and side view time resolved images which were collected using a standard video camera, a VCR, and a monitor, and are shown in the end view of Fig. 2. The side view was often illuminated by a laser sheet emitted from an 8 W Coherent CR-8 Supergraphite Argon Ion Laser. The visual data were analyzed on a high resolution monitor with a superimposed calibrated scale, using the slow motion capabilities of the recorder.

3 New boundary layer observations

A major discovery made during this investigation is that as a Typical eddy convects over the wall, it causes an interaction that results in the formation of a pair of long streaks. If the Typical eddy is convecting towards the wall, when it gets close enough, it will create a pocket, and have one of four types of interactions defined below. The creation of the long streaks occurs even when the Typical eddies are quite distant from the wall, well into the log region.

Observations mentioned above have indicated that hairpin vortices can form as a result of pocket evolution and as a result of lumping instability of existing low speed streaks. We have now identified another mechanism that can result in the formation of hairpin vortices. When a Typical eddy is moving away from the wall at a shallow angle and when it is moving relatively slowly, say $U_c/U_\infty < 0.4$, it will create a pair of long very stable streaks that trail behind a hairpin vortex that lifts-up slowly. The eddy can be as far from the wall as indicated above, and thus, will convect appreciably downstream before the hairpin will be noticed. It may convect out of a field of view, leaving the observer with the impression that the formation of the hairpin did not involve the coherent motion.

Thus, only one coherent motion – interacting with the wall – is necessary to create the long streaks, the pockets and the hairpins. Since all of the remaining structure found in the wall region is related to these structures, we can say that the Typical eddy is responsible for the onset of the turbulent production process.

4 Vortex ring/moving wall simulation of the turbulence production process

We can simulate the interaction of a Typical eddy with the wall region of a turbulent boundary layer by creating a vortex ring and having it convect towards a moving wall. Both the wall and the ring move in the same direction. Figure 3 shows the basic idea behind the simulation. The vortex ring can be aimed at or away from the wall at shallow angles.

To interpret the results of the vortex ring/moving wall interactions in terms of turbulent boundary layer interactions, we must perform a Galilean transformation on the velocity field. Our interpretation of the simulation has been to identify the Stokes' layer with the viscous wall region which extends to y^+ approximately 30–50. The mean velocity at this height is approximately 70–80% of U_∞. Thus,

$$U_{TE}/U_\infty = a\,(1 - U_r/U_w)$$

where a represents the outer region velocity defect which we cannot simulate (20–30%). Thus, in thinking about the implications for the turbulent boundary layer, basically high speed ratios in the simulations correspond to low convection velocities of the Typical eddies in the boundary layer.

As a result, we expect the Typical eddies that emerge from wall layer fluid (through a pinch-off of lifted hairpin vortices, for example) to have a low convection velocity. Since these are moving away from the wall, they will correspond to fast rings moving away from the wall. These exhibit long streak formation which is stable, and pinch-off, depending upon the thickness of the wall layer. We do see long stable low speed streaks in the boundary layer, and we have limited evidence of hairpin pinch-off. On the other hand, Typical eddies that are convecting towards the wall will be of relatively high speed, and thus simulated by low speed vortex rings moving towards the wall.

The Reynolds numbers based upon the initial ring velocity and diameter of the dyed ring bubble, D, ranges between 900 and 2000. When created away from walls, these rings remain stable to azimuthal instabilities over

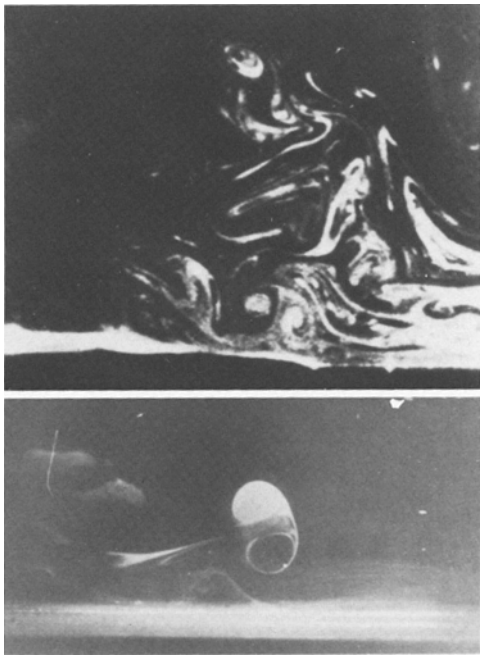

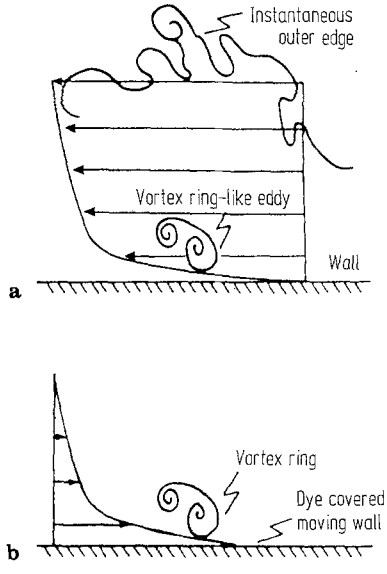

Fig. 3a and b. The basic idea behind the simulation. Performing a Galilean transformation on the vortex ring/moving wall interaction makes it a model of the turbulent boundary layer production process; **a** instantaneous turbulent boundary layer; **b** simulated vortex ring/wall shear layer

durations longer than those used in the interaction experiments.

5 Vortex ring/moving wall interactions

We will describe the model in terms of the velocity ratios and spatial relationships of the simulation. Later in the discussion, we will invoke the Galilean transformation to relate the findings to the turbulent boundary layer case.

5.1 Fast rings ($U_r/U_w > 0.45$) moving towards the wall

Interactions which result from these rings have been described by Liang et al. (1983). They result in the formation of a pocket, and varying degrees of lift-up of wall layer fluid. The interactions have been divided into four types. Figure 4 shows sketches of the four types of interaction. Type I results in a minor rearrangement of the wall layer fluid; followed by the ring moving away from the wall essentially undisturbed. Type II results in a well defined lift-up of wall layer fluid, which takes on a hairpin configuration. This fluid does not get ingested into the ring, and the ring moves away from the wall perturbed, but still a stable ring. The hairpin has been observed to pinch-off, or just move back down towards the wall and dissipate. Type III results in a lifted hairpin of wall layer fluid which gets ingested into the ring, resulting in a chaotic breakdown of both the lifted hairpin and the vortex ring, as the vortex ring is moving away from the wall. Type IV also initiates a hairpin vortex, but in this case the hairpin vortex is ingested into the ring on a much shorter timescale, and the ring and lifted wall layer fluid both breakdown while the ring is very close to the wall.

Liang et al. (1983) used vortex rings with $D^+ > 250$ and δ^+ between 20 and 50, and they observed only the above four types of interactions. Our experiments indicate that if $D^+ < 150$ and δ^+ is between 20 and 50, we can also obtain the four types of interactions noted above, but, in addition, we found that long streaks also formed. In these cases, a hairpin grew out of the open end of the pocket, its legs stretched and a pair of streamwise streaks formed alongside the hairpin legs. The streaks grew to several hundred wall units. This observation is in contrast to the suggestions of a number of investigators that a lifted hairpin vortex would induce a single streak to form between its legs.

5.2 Slow rings ($U_r/U_w < 0.35$) moving towards the wall at a shallow angle

These initial conditions result in a pair of long low speed streaks, $x^+ = O(1{,}000)$, a pocket, and hairpins which induce themselves and portions of the streaks to lift-up.

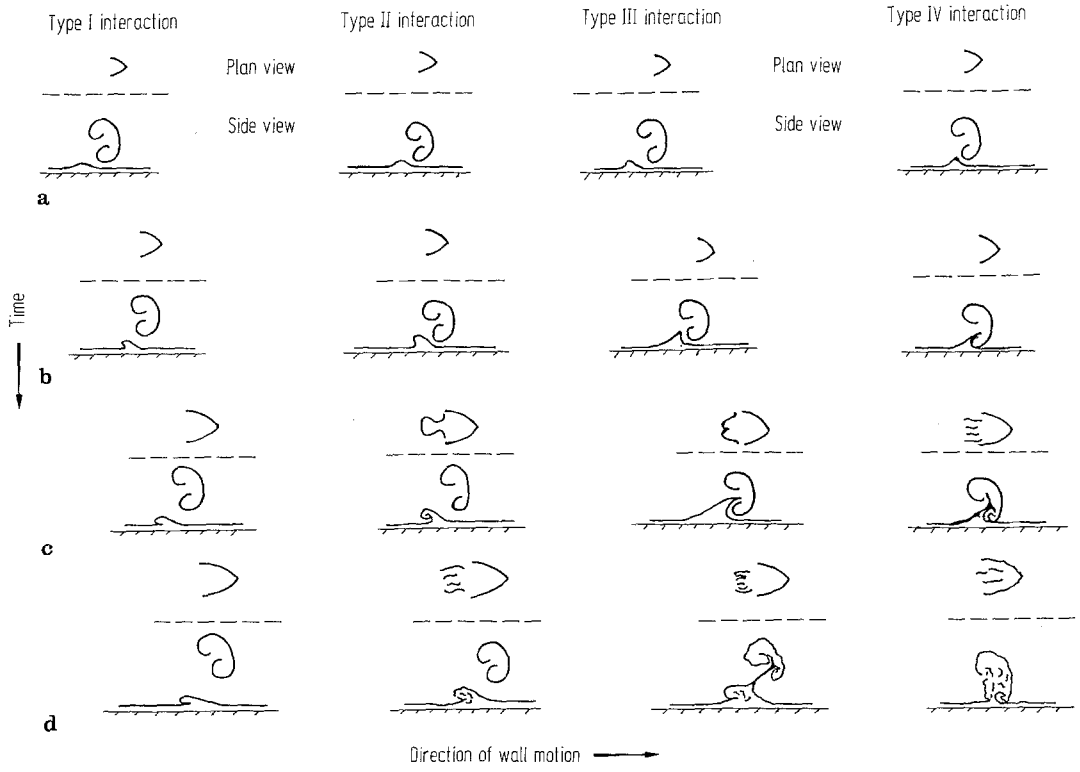

Fig. 4a–d. Sketches of the four types of local vortex ring/moving interactions (see text for explanation)

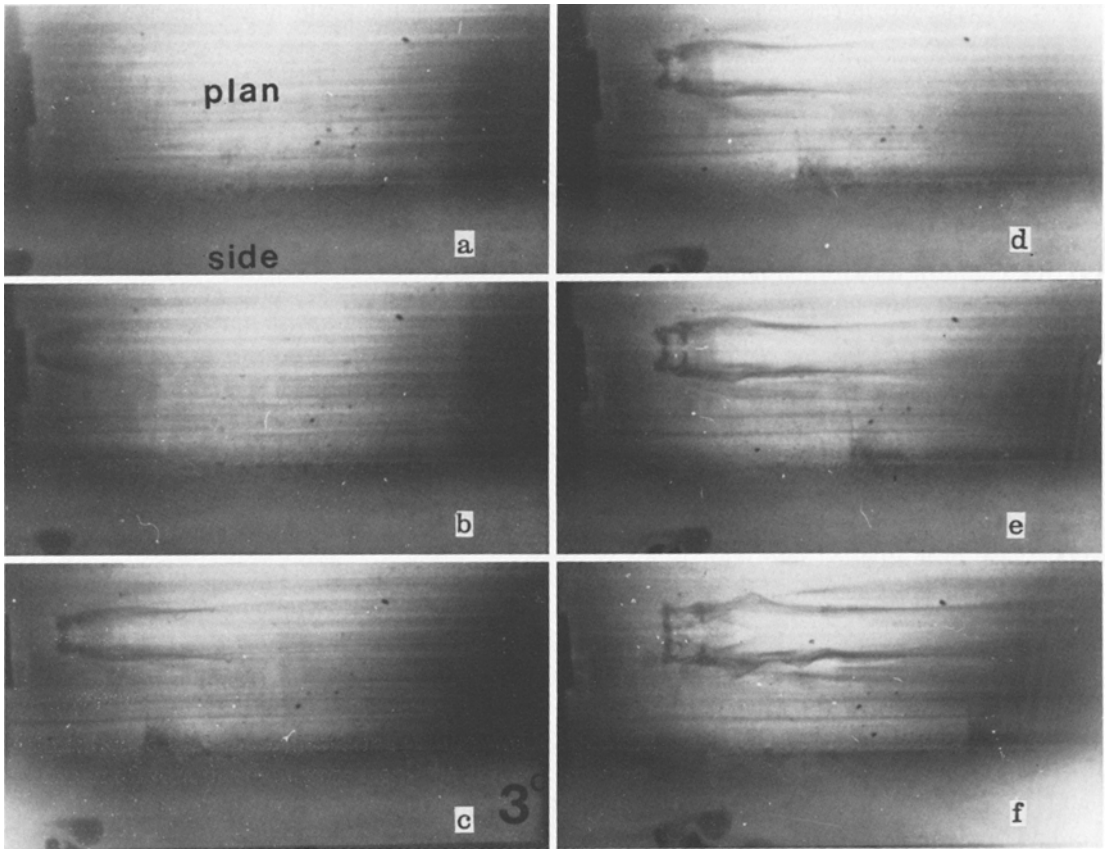

Fig. 5 a – f. Six photos of a vortex ring/moving wall interaction for $U_r/U_w < 0.35$ when the ring moves toward the wall at a 3° angle; Both plan and side views are shown, the ring and the wall are moving to the right, only the wallward side of the ring has dye in it; The interaction results in a pair of long streaks prior to the onset of a pocket and its associated hairpin lift-up, which then gets partially ingested into the ring

Figure 5 shows six photos of this happening prior to the onset of a Type III interaction. We can see the formation of the pair of low speed streaks, followed by the formation of the pocket, and the associated hairpin kift-up, then partial ingestion of the pocket hairpin. The ring later breaks up. The streaks that form under these conditions become wavy and slowly breakdown resulting in additional lift-up and transport. Hairpins have been observed to form over these streaks. The initial conditions are two-dimensional. The moving belt is started from rest, so that the layer approximates a Stokes' layer. These streaks have obviously not formed as the result of the pre-existence of streamwise vortices, but spanwise vorticity has been distorted to give a streamwise component, and it is clear from the Navier Stokes equations that new streamwise vorticity has also been generated at the wall.

5.3 Fast rings ($U_r/U_w > 0.45$) moving away from the wall at a shallow angle (less than 3°)

These initial conditions result in a hairpin vortex which is linked to the distributed streamwise vorticity that has formed a pair of long, very stable, low speed streaks. A pocket is not observed. The evolution of the hairpin in this case has been observed to lead to the pinch-off of this hairpin, forming a vortex ring, and another hairpin. Figure 6 shows four photos of the evolution leading to the creation of a new vortex ring. The long stable streaks which form come closer and closer together, indicating that the streamwise vorticity which caused them, and which is of opposite sign, is being stretched and brought very close together. Diffusion is accelerated, and the vorticity is redistributed into a vortex ring and a hairpin loop. Figure 7 shows long, very stable streaks and a long stretched hairpin which does not pinch-off over the distance available due to size limitations of the experimental facility – more than 2500 wall layer units. There are two initial conditions that may cause this kind of long stretched streamwise vorticity to evolve into a hairpin: (1) δ/D is very small; (2) the ring is far away from the wall. Further study concerning the effects of ring to wall distance is needed.

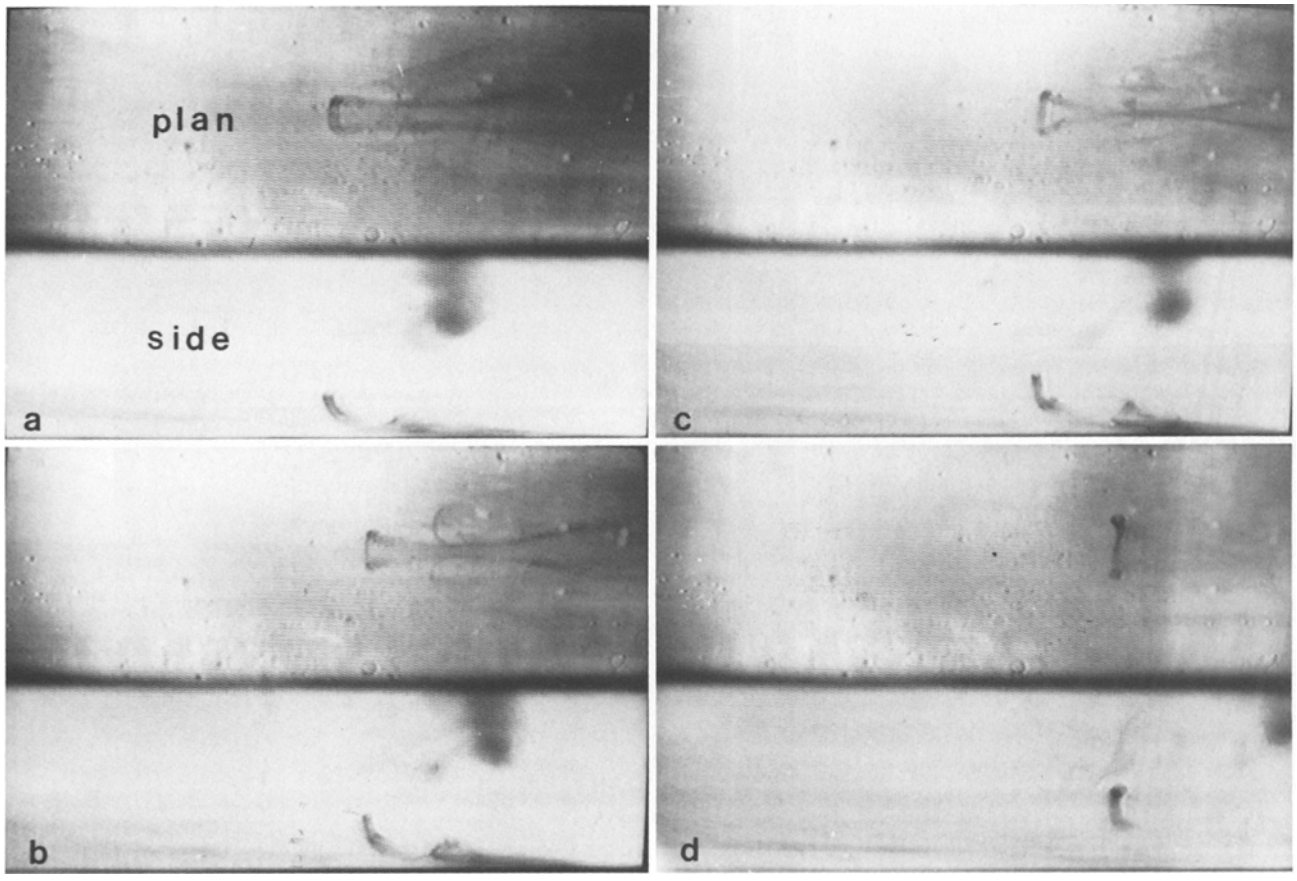

Fig. 6a – d. Four photos of a vortex/ring moving wall interaction for $U_r/U_w > 0.45$ when the ring is moving away from the wall at a 2.5° angle; Both plan and side views are shown, the ring is at the upper right of the side view; ring and wall are moving to the right; A hairpin forms when the interaction starts; the long stable streamwise streaks which also form, come closer and closer together, indicating that the streamwise vorticity which caused them, and which is of opposite sign, is being stretched and coming closer together; this evolution leads to 'pinch-off' and the creation of a new vortex ring

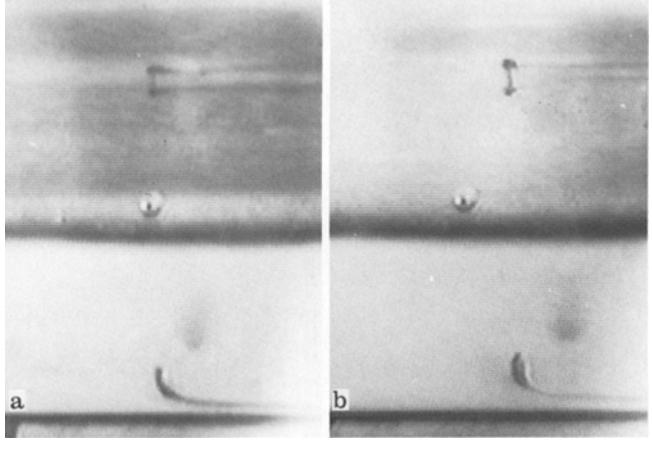

Fig. 7a and b. Same conditions as Fig. 6, except that the wall layer is very thin, so δ/D is small; We obtain long very stable streaks and a long stretched hairpin which does not pinch-off over the 2,500 wall layer distance of the facility; the time between each photo is approximately 50 wall units

5.4 Slow rings ($U_r/U_w < 0.45$) moving away from the wall at a shallow angle

These initial conditions result in a hairpin from which a pair of long, stable, low speed streaks emerge. A pocket is also not observed. The phenomena of hairpin pinch-off, for this case, appears to depend upon δ/D. If $\delta/D < 0.15$ we get pinch-off, but only a part of the fluid involved in the hairpin is observed to pinch-off and form the ring. If δ/D is greater, and the ring moves away from the wall without ingesting any wall layer fluid (Type I or II), the lifted hairpin appears to do very little. Figure 8 shows four photos of the evolution for $\delta/D > 0.15$. In this case a pocket does not form, and it appears that the hairpin has been generated by the initial vortex ring/wall interaction, and that a pair of streamwise vortices – which could be called its legs – trail behind, creating the streak pair. Pinch-off does not occur. Figure 9 shows four photos of the interaction for $\delta/D < 0.15$. In this case pinch-off of a

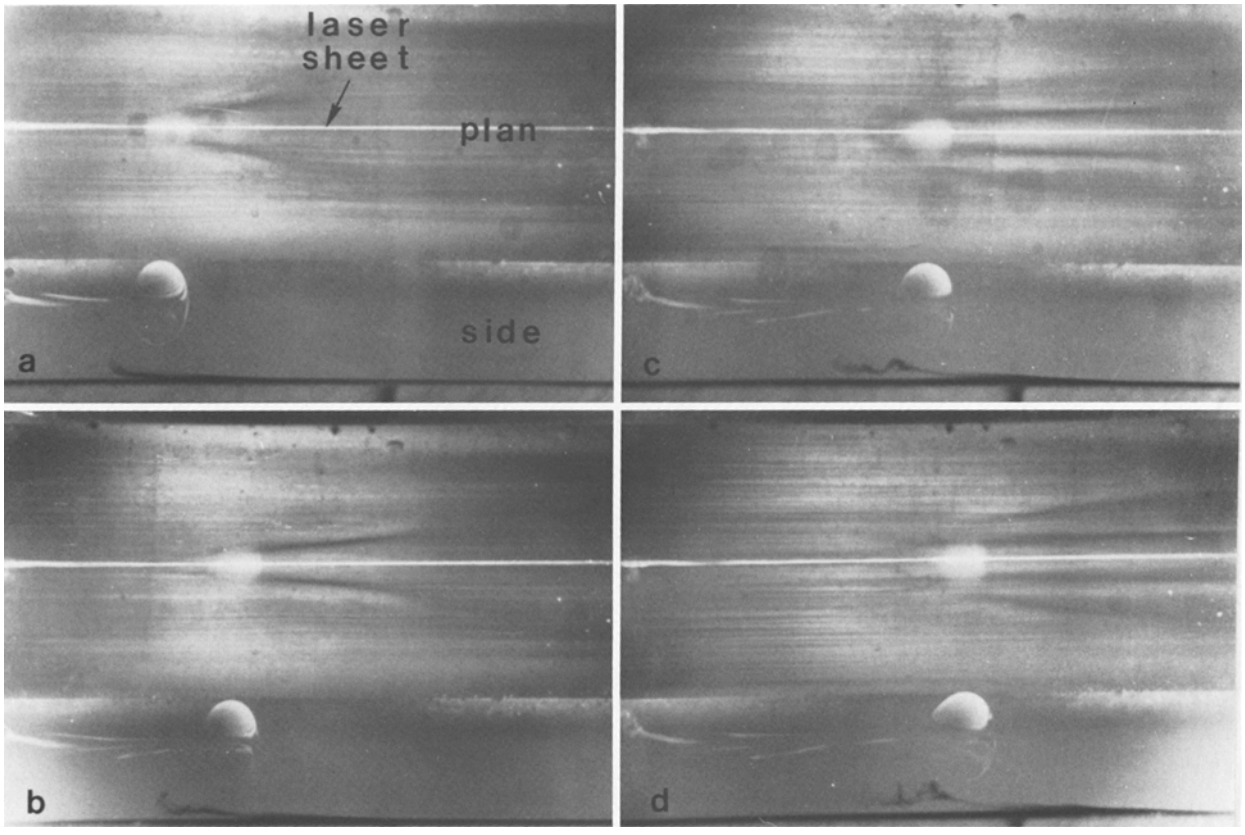

Fig. 8a–d. Four photos of a vortex/ring moving wall interaction for $U_r/U_w < 0.45$ when the ring is moving away from the wall at a 2.5° angle and $\delta/D > 0.15$; Both plan and side views are shown; the ring has most of its dye in the upper part, ring and wall are moving to the right; Again a pair of long stable streaks is created, a pocket does not form, and a weak hairpin which forms does not pinch-off; there is evidence of a second pair of streaks forming

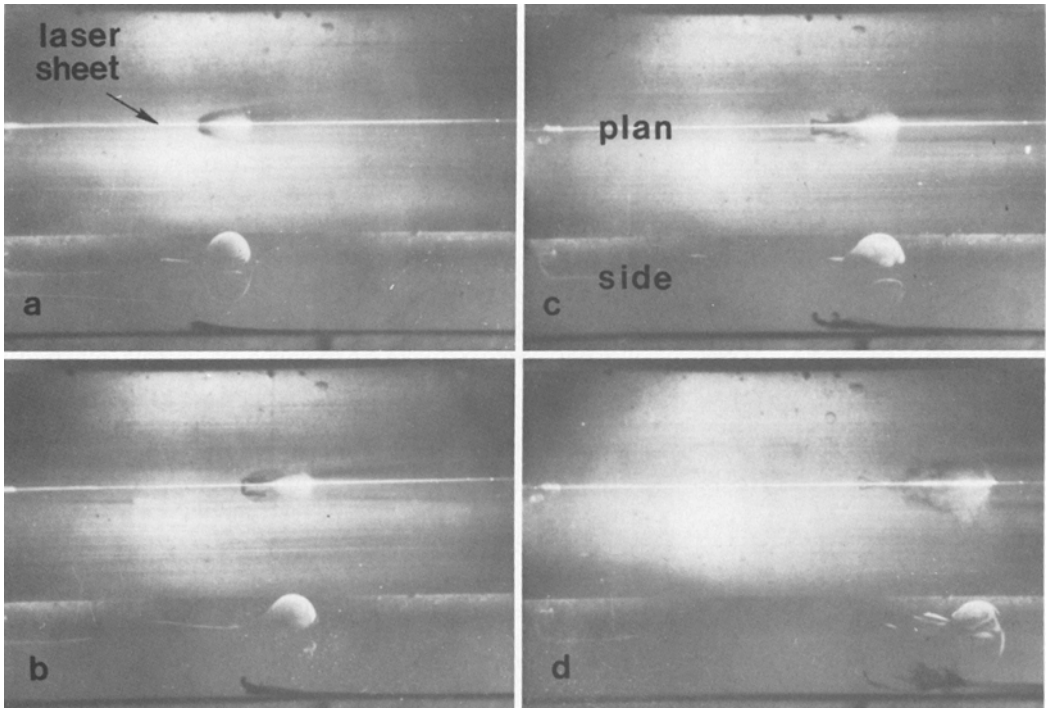

Fig. 9a–d. Same conditions as Fig. 8, except that $\delta/D < 0.15$; in this case we again obtain a pair of long stable streaks and a hairpin; Pinch-off of a portion of the lifted hairpin does occur creating a new small vortex ring; We don't have the secondary streak pair forming

portion of the lifted hairpin does occur, creating a new small vortex ring.

5.5 Summary of interactions

We have found that for rings moving towards the wall at 3°, the formation was not a function of δ/D, for $D^+ > 250$. The form taken was a function of U_r/U_w; long streaks and pockets formed for $U_r/U_w < 0.35$, short streaks and pockets when $0.35 < U_r/U_w < 0.45$, and only pockets for higher speed ratios. For rings moving away from the wall at 2.5°, long streaks are generated over the entire speed ratio range studied, and δ/D now plays an important role. When $U_r/U_w < 0.55$, if δ/D is less than 0.15 we get long streaks and pinch-off of a small hairpin. For $\delta/D > 0.15$, we don't get pinch-off. In the range $0.55 < U_r/U_w < 1$, if $\delta/D > 0.05$ we get long streaks and hairpin pinch-off, for smaller values of δ/D we have a long stretched hairpin and pinch-off is not observed.

5.6 Scaling associated with the vortex ring/moving wall interactions

From our perspective of a turbulence production model, the streak spacing, streak length and wavelength of the streak instability are quantities of interest.

The dependence of the streak spacing in wall units on the size of the vortex ring in wall units, for an incidence angle of 3° and $U_r/U_w = 0.31$, is shown in Fig. 10. The thickness of the wall layer (in wall units) is shown next to each data point. The streak spacing, Z^+, is within 10% of the ring diameter for wall layer thicknesses between 20 and 50 wall units. Results show that decreasing U_r/U_w will decrease the average streak spacing relative to the ring size for fixed incidence angles. Furthermore, increasing the incidence angle of the vortex ring will increase the average streak spacing for a given ring size and speed ratio. Figure 11 shows the dependence of the streak spacing on the speed ratio and angle.

Measurements show that streak lengths greater than $x^+ \cong 500$ were obtained for many of the interactions in ranges where the streaks are stable (for rings with $D^+ = 100$, streaks as long as $x^+ = 1{,}000$ were found).

Figure 12 shows the non-dimensionalized streamwise wavelength that sets in as a function of δ^+ for different U_r/U_w. The wavelength is the same order as the ring diameter. It decreases as the ring/wall speed ratio.

5.7 Stability considerations

Some additional data has been obtained, which confirms and extends the results of Liang (1984), showing that the boundary between stable ring wall interactions (Types I and II), and unstable interactions (Types III and IV)

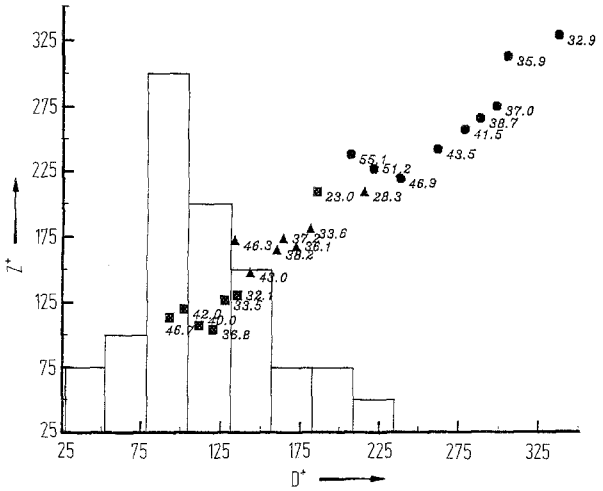

Fig. 10. The distribution of D^+ obtained from the diameter of the Typical eddies of a turbulent boundary layer at $R_\theta = 1{,}176$, superimposed upon the streak spacing obtained for various size rings, for an incidence angle of 3° and $U_r/U_w = 0.31$; the thickness of the wall layer (in wall units) is shown next to each data point

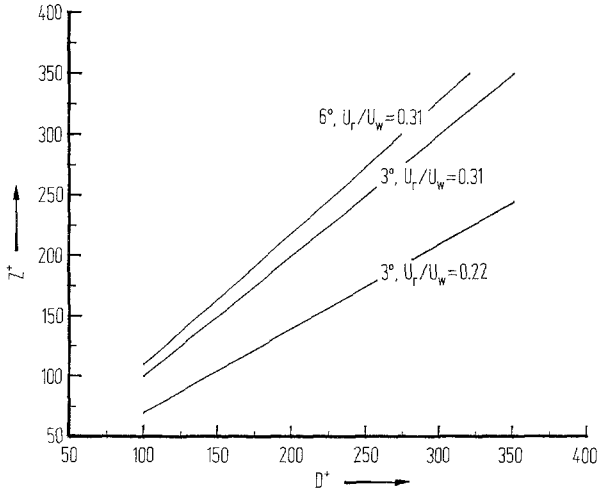

Fig. 11. The dependence of the streak spacing on the speed ratio and ring interaction angle

depends upon δ/D. Figure 13 shows a stability map of the interactions for 3° rings. We can see that for low ring/wall speed ratios, the ring stability depends primarily upon the relative thickness of the wall layer and the size of the ring; for thicker wall layers or smaller rings, the interactions are more stable. Furthermore, the shallower the incidence angle, the more stable the interaction.

Figure 14 shows the dependence of the time to instability of the streaks which exhibited wavy instability on the wall layer thickness (both quantities non-dimensionalized by wall layer variables) for 3° incidence rings. We can see that for each convection velocity ratio, there is a value of δ^+ above which the time to instability becomes much longer. As the ring/wall speed ratio increases, the critical

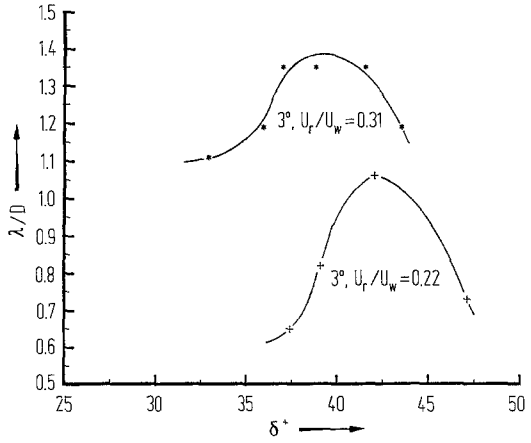

Fig. 12. The non-dimensionalized streamwise wavelength of streaks subjected to wavy instabilities

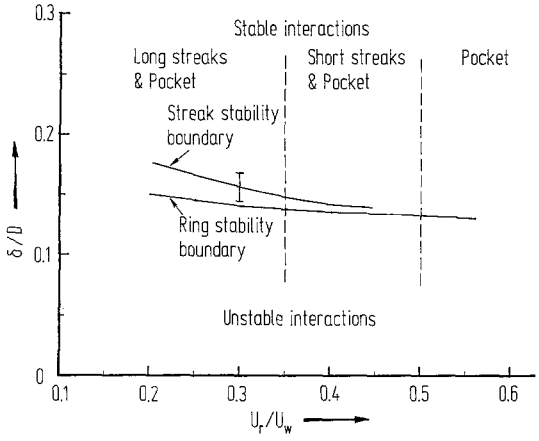

Fig. 13. Comparison of the 'stability boundaries' of a three degree ring moving towards the wall, and of the stability boundaries of the streaks those same rings create; the ring stability boundaries and the streak stability boundaries for different size rings collapse when plotted this way

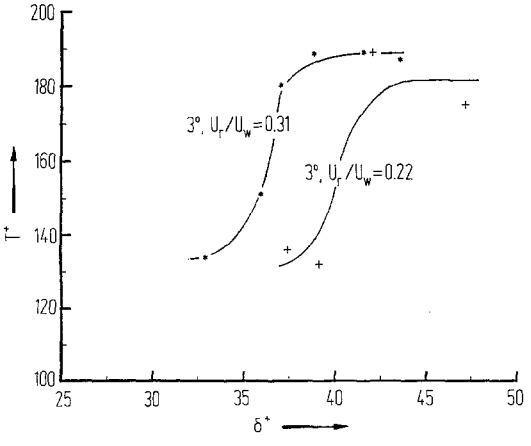

Fig. 14. The dependence of the time to instability of the streaks on the wall layer thickness (both quantities non-dimensionalized by wall layer variables) for 3° incidence rings

thickness of the wall layer needed to increase the time to instability decreases.

Both the rings and the streaks are more stable when the wall layer is thicker. Figure 13 shows a comparison of the stability boundaries of a three degree ring moving towards the wall, with the stability boundary of streaks formed by those same rings. The streak stability boundary has generally the same shape; stable rings will, in general, correspond to stable streaks, except for a small range of δ/D. The ring stability curves and the streak stability boundary curves for different size rings collapse when plotted this way.

The streak stability boundary represents the boundary between conditions that will enable a pair of long streaks to form. For δ/D below the boundary, we have a very unstable situation in which the fluid in the region around the eddy seems to rearrange itself into the beginnings of a streak, but the streak is not stable, and immediately breaks up. For δ/D values above the boundaries, a pair of long streamwise streaks form. However, once formed, the streaks are susceptible to breakdown as noted above, where the time to instability is a function of angle, convection velocity, and the instantaneous wall layer thickness (for example, Fig. 14).

6 Implications for turbulent boundary layers

By performing a Galilean transformation on the simulation, we recover the essential aspects of the Typical eddy wall region interaction in a turbulent boundary layer flow. The wide range of interactions that can be simulated using the vortex ring/moving wall experiments are not all admitted by the turbulent boundary layer with equal frequency. Some are not admitted at all. The range of the parameters (angle, wall layer thickness, convection velocity) found in the boundary layer are limited, and in all cases they have skewed probability distributions (towards higher values) that are approximately lognormal. When these distributions are used to determine the events that are most probable, we begin to see what to expect.

The distribution of D^+ obtained from the diameter of the Typical eddies of a turbulent boundary layer at $R_\theta =$ 1,176 is also shown in Fig. 10, superimposed upon the streak spacing obtained for various size rings. When the simulation outcomes are conditioned by the probabilities of scales found in this boundary layer, we see that the simulation gives a most likely streak spacing of approximately 100 wall units. This is an important quantitative test of the quality of the simulation, for although the average streak spacing is $\lambda^+ \cong 100$, all observations of streak pairs have also shown their spacing to be approximately this value.

6.1 Implications for drag modifications

As we have seen, small changes in the parameters of Typical eddy size, incidence angle, convection velocity, and wall layer thickness can alter the evolutions that result when a Typical eddy interacts with the wall. Changes in any of these variables which cause a crossover in the stability boundaries will result in a change in the drag at the wall.

Consider, for example, the angle of incidence. If we can change the strength of the large scale motions, say, by outer layer manipulators, we can easily change the angle of a Typical eddy that is moving towards – or away from – the wall, and may even be able to change the direction. This will affect the stability of both the local eddy wall interaction (interactions of Type I–IV), and the stability of the streaky structure which is created, as well as the formation of new Typical eddies via the pinch-off process. Thus, we can affect not only the local drag, but alter the drag downstream by directly interfering with the cyclic production process.

Modifications to the wall that result in small changes in the effective wall region thickness, for example. NASA riblets, will also have an effect on the drag. If increases in wall region thickness above the critical thickness can be made (for example, Fig. 13), streaks are more likely to remain stable. Furthermore, the local interactions (Types I–IV) will also tend to be of Type I and II. Thus, the drag can also be reduced.

7 Conclusions

New findings in the turbulent boundary layer have suggested that long, low speed streaks are formed in pairs as the result of the interactions of microscale very coherent vortex ring-like eddies (Typical eddies) propagating over the wall.

The vortex ring/moving wall simulation of the turbulence production process was shown to incorporate all of the evolutions, interactions, and structural features. It dramatically demonstrates that streamwise vortices are not required to produce streamwise streaks. When the streak spacings obtained in the simulation are conditioned by the probability of occurrence of Typical eddy scales found in the boundary layer, we see that the simulation provides the correct streak spacing (approximately 100 wall units). Other possible outcomes of the simulation need to be weighed by the measured probabilities of occurrence of the angles, convection velocities, and length scales of the Typical eddies in the turbulent boundary layer to enable us to obtain a picture of the most probable forms of the interactions, and to gain insight into the causes of the interactions which occur with lower probability, that may contribute significantly to the transport. It appears that turbulent boundary layer control leading to drag reduction can be realized by fostering the conditions suggested by the simulations which will increase the probability of having stable interactions.

Acknowledgements

This research was sponsored by the Air Force Office of Scientific Research under Contract No. F49620-85-C-0002. We would like to thank Dr. J. McMichael for his encouragement and advice as contract monitor.

References

Acarlar, M. S.; Smith C. R. 1984: An experimental study of hair-pin-type vortices as a potential flow structure of turbulent boundary layers. Rept. FM-5, Dept. of M.E./Mech., Lehigh Univ.

Falco, R. E. 1974: Some comments on turbulent boundary layer structure inferred from the movements of a passive contaminant. AIAA Pap. 74–99

Falco, R. E. 1977: Coherent motions in the outer region of turbulent boundary layers. Phys. Fluids 20, S124–S132 (Suppl. II)

Falco, R. E. 1980a: The production of turbulence near a wall. AIAA Pap. No. 80–1356

Falco, R. E. 1980b: Structural aspects of turbulence in boundary layer flows. In: Turbulence in liquids (ed. Patterson, G. K.; Zakin, J. L., pp. 1–15. Dept of Chemical Engineering, Univ. of Missouri-Rolla

Falco, R. E. 1980c: Combined simultaneous flow visualization/hot-wire anemometry for the study of turbulent flows. J. Fluids Eng. 102, 174–183

Falco, R. E. 1982: A synthesis and model of wall region turbulence structure. In: The structure of turbulence, heat and mass transfer (ed. Zoric, Z.), pp. 124–135. Washington: Hemisphere

Falco, R. E. 1983: New results, a review and synthesis of the mechanism of turbulence production in boundary layers and its modification. AIAA Pap. No. 83-0377

Head, M. R.; Bandyopadhyay, P. 1981: New aspects of turbulent boundary layer structure. J. Fluid Mech. 107, 297–337

Kim, J. 1986: Investigation of turbulent shear flows by numerical simulation. Tenth Congress of Applied Mechanics, Austin TX, June 16–20

Liang, S. 1984: Experimental investigation of vortex ring/moving wall interactions. MS thesis, Dept. Mech. Eng. Michigan State Univ.

Liang, S.; Falco, R. E.; Bartholomew, R. W. 1983: Vortex ring/moving wall interactions: experiments and numerical modeling. Bull. Am. Phys. Soc. Ser. II, 28, 1397

Moin, P.; Leonard, A.; Kim, J. 1986: Evolution of a curved vortex filament into a vortex ring. Phy. Fluids 29, 955–963

Oldaker, D. K.; Tiederman, W. G. 1977: Spatial structure of the viscous sublayer in drag reducing channel flow. Phy. Fluids 20, 133–144

Praturi, A. K.; Brodkey, R. S. 1978: A stereoscopic visual study of coherent structures in turbulent shear flow. J. Fluid Mech. 89, 251–278

Runstadler, P. W.; Kline, S. J.; Reynolds, W. C. 1963: An experimental investigation of the flow structure of the turbulent boundary layer. Dept. of Mech. Eng. Rep. MD-8, Stanford Univ.

Smith, C. R. 1982: Application of high speed videography for study of complex, three-dimensional water flows. SPIE 348, High Speed Photography (San Diego), pp. 345–352

Smith C. R.; Metzler, S. P. 1983: The characteristics of low-speed streaks in the near-wall region of a turbulent boundary layer. J. Fluid Mech. 129, 27

Received September 8, 1987